TRAJEVAE - Controllable Human Motion Generation from Trajectories
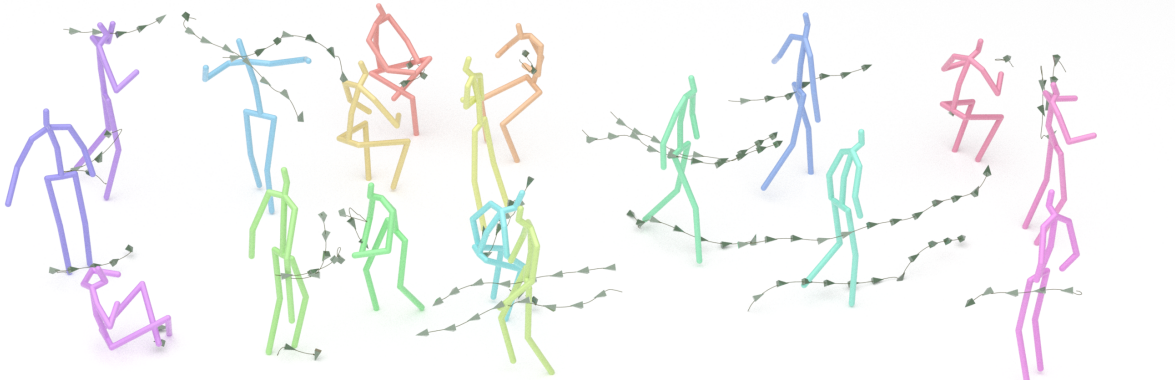
Kacper Kania[1]   Marek Kowalski[2]   Tomasz Trzciński[1,3,4]

[1]Warsaw University of Technology
[2]Microsoft
[3]Tooploox
[4]Jagiellonian University

Figure 1. TRAJEVAE transforms 3D trajectories into a plausible human animation. The model requires only an initial pose and any number of input trajectories for each character in a scene. Generated animations can be composed to create vivid animated scenes.

Abstract

The generation of plausible and controllable 3D human motion animations is a long-standing problem that often requires a manual intervention of skilled artists. Existing machine learning approaches try to semi-automate this process by allowing the user to input partial information about the future movement. However, they are limited in two significant ways: they either base their pose prediction on past prior frames with no additional control over the future poses or allow the user to input only a single trajectory that precludes fine-grained control over the output. To mitigate these two issues, we reformulate the problem of future pose prediction into pose completion in space and time where trajectories are represented as poses with missing joints. We show that such a framework can generalize to other neural networks designed for future pose prediction. Once trained in this framework, a model is capable of predicting sequences from any number of trajectories. To leverage this notion, we propose a novel transformer-like architecture, TRAJEVAE, that provides a versatile framework for 3D human animation. We demonstrate that TRAJEVAE outperforms trajectory-based reference approaches and methods that base their predictions on past poses in terms of accu-

racy. We also show that it can predict reasonable future poses even if provided only with an initial pose.

1. Introduction

Reproducing realistic real-life human animation is one of the key components in robotics, game, and movie industries. Typically when producing an animation, the animator starts with defining a character's skeleton. Parts in these skeletons are created to be in a specific, manually defined relation such that each joint influences the position of a subset of other joints in a *kinematic chain* which integrates these relations over all joints. While these relations are helpful to maintain skeleton movement constraints, they are not sufficient to create realistic animation. The generation of such animations is, in fact, a complex task that requires the animator to manually key-frame the joint positions throughout the sequence. While *inverse kinematics* methods [55, 5] can aid this procedure, their priors are not strong enough to ensure that the motion is realistic, especially when only a few joint positions are known. Alternatively, the animation sequence can be pieced together from shorter motion-captured sequences. However, the capture of such sequences is costly and time-consuming [27].

The automation of character animation is a long-standing problem with multiple solutions proposed, including those based on neural networks and probabilistic models [57, 58, 62, 17, 30, 29]. The main goal of these methods is to generate sequences of joint positions given some conditioning information. More recent approaches can be split into two categories: methods conditioned on the past motion or those conditioned on a single control signal. The former methods generate future motion based on a set of past frames [17, 44, 64, 68, 7, 15, 23, 70, 71, 74, 47]. However, they suffer from two limitations: they do not provide any control over generated future poses and generate future motions only when past frames of the full-body are provided.

The latter methods generate motion from a *control signal* [25]. This control signal can be any partial future information, for example, the direction of the movement, speed, type of an action being performed, coordinates of a particular joint, or any combination of the above [25, 52, 12, 18, 28, 72, 66]. However, these methods can handle only simple motions a body, such as walking, running, or side-stepping, and cannot generate fine-grained motions of each of the joints. In many cases, this formulation becomes impractical, *e.g.* when simulating a crowd scene where characters perform vivid actions such as jumping, bending, or hand waving, as shown in Fig. 1. It is not straightforward to extend those methods to incorporate more information, as feasible computational cost and convergence of the resulting models are not guaranteed.

To mitigate these issues, we propose a data-driven approach to train a model to handle a variable number of pieces of information, *trajectories*, for human motion generation. A single *trajectory* refers to a particular pose joint and specifies where that joint should be located in each time step. We can choose whether we want to specify trajectories of a few joints and leave the rest to be generated by the model or generate a more specific motion by adding more trajectories. This formulation introduces an unprecedentedly flexible framework that encompasses all previous approaches while offering adjustable control over the generated motion.

We formulate the problem of predicting future poses from trajectories as a *pose completion* problem. We trace the inspiration for that formulation to the evolutionary cognitive skills of humans who are able to *hallucinate* [34] the rest of a human body out of a few markers that exhibit a human motion. While a similar formulation was firstly used in [26], it was applied to a significantly different task of predicting future motions from past frames. Similarly, [37] predicts missing poses in a sequence where only some of pose frames are given. Since we cast our problem as a structured *pose completion*, we leverage recent advancements for stochastic tensor completion [75] and show the application of that paradigm on a novel motion generation model which

we call TRAJEVAE. Thanks to our formulation, we achieve a desirable property that the accuracy of generated motions increases when more information is provided at the input. At the same time, our model can predict future poses even if no trajectory is given. In industrial applications, our method can generate full-body animations for automatically-tracked joints while naturally handling missing information if some of the joints are not seen by the model. TRAJEVAE outperforms trajectory-based baselines and methods based on several past full body frames in terms of accuracy.

We summarize our contributions as follows:

- We present a simple and general training paradigm that enables controllable generation of future poses from a variable number of input information pieces.

- We introduce TRAJEVAE — the first generative model that predicts diverse poses from any number of input trajectories.

- We empirically show that thanks to our formulation existing methods for generating motion from a single trajectory can be adapted to use multiple trajectories.

2. Related Works

Deterministic motion prediction In recent years, multiple methods were proposed for predicting a single future motion based on a corresponding past sequence of poses [3, 2, 11, 13, 19, 22, 21, 23, 42, 43, 48, 47, 49, 54, 52, 61] or video frames [49, 17, 53, 73, 35, 32]. Cai *et al.* [11] and Aksan *et al.* [2] use a transformer-like architecture to achieve this goal. Mao *et al.* [48, 47] extend the pose representation by performing Discrete Cosine Transform (DCT) [1] on joint coordinates. They additionally applied Graph Convolutional Networks (GCN) to incorporate the spatial information relationships between joints. Lebailly *et al.* [41] adapted inception modules [60] to handle different temporal resolutions of the data. While being successful, these methods are limited to predicting a single future pose sequence.

Stochastic motion prediction To model the distribution of possible motions, recent works [68, 64, 24, 45, 26, 4, 71, 40, 37, 33] leverage advances for generative modeling and build upon models such as Generative Adversarial Networks (GANs) [20], Variational Autoencoders (VAEs) [39] or normalizing flows [56]. These models enable sampling multiple future pose sequences and to accomplish this, they are often built as conditional models (CGANs [20] and CVAEs [39]). Barsoum *et al.* [7] use Wasserstein GAN [6] in a sequence-to-sequence framework. To make poses more realistic, they regularize bone lengths and deviations between poses in consecutive frames. Walker *et al.* [64] apply VAE for the same goal and uses predicted poses to generate structurally consistent images. Similar to our approach,
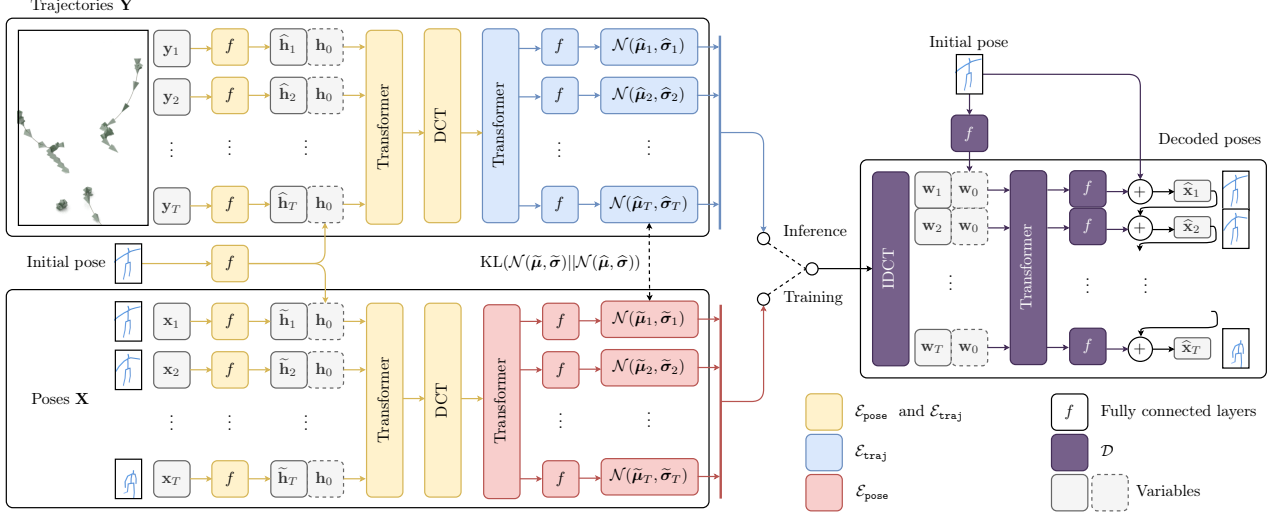
Figure 2. **Pipeline** of our TRAJEVAE architecture trained in the *pose completion* paradigm. TRAJEVAE completes the sequence of missing joints and allows us to generate diverse poses from a variable number of input trajectories. During inference, we drop the part responsible for encoding poses **X**.

Ruiz *et al*. [26] treats the motion prediction as a pose completion problem. However, they consider only randomly incomplete data while we train our method explicitly to leverage a variable number of available joint trajectories.

Stochastic prediction from trajectories While the aforementioned approaches achieved remarkable results, they are limited in a fundamental way — their predictions cannot be controlled explicitly. By the explicit control, we express a situation when one draws a trajectory of either the whole body or a particular joint and expects that the generated character will follow that trajectory. This area has developed significantly in recent years [54, 53, 52, 25, 28, 12, 59, 72, 16]. Nevertheless, such methods are trained to handle a single trajectory, often represented as a target pelvis coordinate projected onto the floor's plane, or as a tuple of velocities for each axis. Pavllo *et al*. [54] encode a control signal in the form of the desired trajectory. Henter *et al*. [25] input to the model a t control signal and past control signals to predict $t + 1$ pose. Holden *et al*. [28] split the motion into phases and model them with a phase-conditioned neural network. Yet these approaches are designed for a single trajectory and cannot generate motions like jumping jacks or hand waving where multiple trajectories need to be specified.

Image completion Image completion or image inpainting [8] is a well-known problem in computer vision. We posit that some of the already proposed approaches [46, 10, 50, 67, 69] can be successfully applied for pose completion where only a part of the pose is given. Liu *et al*. [46] defines a partial convolution where the image is convolved only over pixels that are available in the input. Yu *et al*. [69] incorporates generative adversarial networks [20] and an attention mechanism to improve overall

results. Zheng *et al*. [75] define a probabilistic model in the VAE framework that allowed them to generate diverse and realistic image completions.

3. Method

We introduce a novel paradigm of the trajectory representation that enables fine-grained motion control with an arbitrary number of joint trajectories. We show that generating full-body poses from trajectories can be treated as a *pose completion* problem. Then, we describe TRAJEVAE that builds on the introduced paradigm and allows us to sample multiple, diverse poses which follow the conditioning trajectories. Throughout the whole paper, we parametrize trajectories and poses in 3D global coordinates. Note, however, that our approach is applicable to other pose representations proposed in the literature, such as relative coordinates [71] and exponential maps [54]. We show the overview of our model in Fig. 2.

3.1. Handling multiple trajectories

We formulate the problem of predicting poses that follow a particular trajectory as a pose completion problem. We denote a trajectory $\mathbf{Y} = \{\mathbf{y}_1, \ldots, \mathbf{y}_T\}$ of length T as vectors with $k \leq J$ known joint positions from a corresponding pose sequence $\mathbf{X} = \{\mathbf{x}_1, \ldots, \mathbf{x}_T\}$, where $\mathbf{x}_t, \mathbf{y}_t \in \mathbb{R}^{3J}$. The trajectories of the unknown $J - k$ joints in $\mathbf{Y}$ are set to 0. The goal of the *pose completion* task is to predict $\mathbf{X}$ given $\mathbf{Y}$.

To mimic real-life scenarios, we randomly mask at the training time some of joints in the input pose, which corresponds to the typical use cases such as occlusions or omissions by the animation artist. At each time step, we sam-

ple a matrix $\mathbf{M} \in \{0,1\}^{T \times 3J}$ that masks the same joints across T time steps. Therefore, trajectories are obtained as $\mathbf{Y} = \mathbf{X} \odot \mathbf{M}$ where $\odot$ is the element-wise multiplication.

We motivate the introduced pose completion paradigm as follows. Firstly, in contrast to all related works that are limited to a single trajectory, our method allows the user to select how many trajectories are supplied to the network. As we show in experiments, this paradigm enables a neural network model to handle a varying number of input trajectories. Secondly, applying standard inverse kinematics becomes non-trivial when many joints are missing, and there is a need for a model that is capable of learning the distribution of plausible poses. Finally, formulating the task as a pose completion allows us to build our solution on recent advancements for stochastic image completion.

3.2. Pose completion with a neural network

To show the applicability of the introduced framework, we design TRAJEVAE — a Conditional Variational Autoencoder (CVAE) [39] with a transformer-like architecture [63, 65], and a learnable prior distribution. The transformer architecture allows us to generate poses of a sequence in parallel while the learnable prior increases the sampling diversity. We draw the inspiration for this architecture from models proposed for image completion and prior learning [75, 14]. Our model is an autoencoder with two encoders $\mathcal{E}_{\text{pose}}, \mathcal{E}_{\text{traj}}$ and a single decoder $\mathcal{D}$, where most of the blocks are shared. $\mathcal{E}_{\text{pose}}$ produces parameters of the posterior distribution q_{pose} from the input poses $\mathbf{X}$. These parameters are optimized to match the trajectory prior distribution p_{traj} parametrized by $\mathcal{E}_{\text{traj}}$. Since we train the model to match distributions q_{pose} and p_{traj}, the decoder $\mathcal{D}$ produces results that are similar for both $\mathcal{E}_{\text{traj}}$ and $\mathcal{E}_{\text{pose}}$. During inference, we do not have access to the ground truth future poses and hence we drop $\mathcal{E}_{\text{pose}}$ that is responsible for encoding poses during training.

Encoding poses and trajectories To take advantage of the similarity between representations of poses and trajectories, parameters of $\mathcal{E}_{\text{traj}}$ and $\mathcal{E}_{\text{pose}}$ are shared unless stated otherwise. We firstly encode the 3D coordinates of $\{\mathbf{y}_t\}_{t=1}^T$ and $\{\mathbf{x}_t\}_{t=1}^T$ with $\mathcal{E}_{\text{traj}}$ or $\mathcal{E}_{\text{pose}}$ to get $\{\widehat{\mathbf{h}}_t\}_{t=1}^T$ and $\{\widetilde{\mathbf{h}}_t\}_{t=1}^T$ respectively. We concatenate them with an initial pose processed by a neural network that produces $\mathbf{h}_0$. $\widehat{\mathbf{H}} = \{[\widehat{\mathbf{h}}_t; \mathbf{h}_0]\}_{t=1}^T$ for trajectories and $\widetilde{\mathbf{H}} = \{[\widetilde{\mathbf{h}}_t; \mathbf{h}_0]\}_{t=1}^T$ for poses are passed to two self-attention layers [63]. Then, we apply the Discrete Cosine Transform (DCT) for each feature in all vectors independently, and obtain vectors $\text{DCT}(\widehat{\mathbf{H}}) \in \mathbb{R}^{T \times (|\widehat{\mathbf{h}}|+|\mathbf{h}_0|)}, \text{DCT}(\widetilde{\mathbf{H}}) \in \mathbb{R}^{T \times (|\widetilde{\mathbf{h}}|+|\mathbf{h}_0|)}$ in the frequency domain. Since DCT operates with an orthogonal basis, the resulting codes are independent of each other. Thus, we can sample them independently, if we assume that they are governed by a defined distribution.

To this point, all parameters for processing trajectories

$\mathbf{Y}$ and poses $\mathbf{X}$ are shared to leverage the fact that trajectories represent masked future poses. We then split the pipeline into two unshared parts — one for trajectories and one for poses — that are composed of transformer-like encoders that facilitate information sharing between the latent codes. The final multilayer perceptrons produce parameters $(\{\widehat{\boldsymbol{\mu}}_t, \ldots, \widehat{\boldsymbol{\mu}}_T\}, \{\widehat{\boldsymbol{\sigma}}_1, \ldots, \widehat{\boldsymbol{\sigma}}_T\})$ of a normal distribution for trajectories, and $(\{\widetilde{\boldsymbol{\mu}}_1, \ldots, \widetilde{\boldsymbol{\mu}}_T\}, \{\widetilde{\boldsymbol{\sigma}}_1, \ldots, \widetilde{\boldsymbol{\sigma}}_T\})$ for poses.

Learnable prior A simple reconstruction of poses $\mathbf{X}$ from trajectories $\mathbf{Y}$ and therefore constraining the latent space to a standard normal distribution $\mathcal{N}(0, I)$, as common in VAEs, is too restrictive and impedes the diversity of generated samples significantly. To overcome the problem and to provide a more flexible distribution, we make the prior learnable [14, 75] and define it as $p_{\text{traj}}(\widehat{\mathbf{z}}_t|\mathbf{y}_1, \ldots, \mathbf{y}_T)$. During training, we match the posterior distribution $q_{\text{pose}}(\widetilde{\mathbf{z}}_t|\mathbf{x}_1, \ldots, \mathbf{x}_T)$ by optimizing the Kullback-Leibler divergence:

$$-\text{KL}(q_{\text{pose}}(\widetilde{\mathbf{z}}_t|\mathbf{x}_1, \ldots, \mathbf{x}_T)||p_{\text{traj}}(\widehat{\mathbf{z}}_t|\mathbf{y}_1, \ldots, \mathbf{y}_T)),$$

where $\widehat{\mathbf{z}}_t \sim \mathcal{N}(\widehat{\boldsymbol{\mu}}_t, \widehat{\boldsymbol{\sigma}}_t)$ and $\widetilde{\mathbf{z}}_t \sim \mathcal{N}(\widetilde{\boldsymbol{\mu}}_t, \widetilde{\boldsymbol{\sigma}}_t)$ are samples from the prior and posterior distributions respectively.

Decoding poses We transform pose latent vectors $\{\widetilde{\mathbf{z}}\}_{t=1}^T$ during training and trajectory latent vectors $\{\widehat{\mathbf{z}}\}_{t=1}^T$ during inference into the original time domain $\{\mathbf{w}\}_{t=1}^T$ with Inverse Discrete Cosine Transform (IDCT) [1]. We additionally encode the initial pose with an MLP to obtain $\mathbf{w}_0$ as we found it improves overall results. A set of concatenated vectors $\{[\mathbf{w}_t; \mathbf{w}_0]\}_{t=1}^T$ is decoded with a self-attention decoder. The final fully connected layers predict offsets $\widehat{\mathbf{o}}_t$ of the reconstructed pose $\widehat{\mathbf{x}}_{t-1}$ from the time step $t-1$. Finally, the reconstructed pose $\widehat{\mathbf{x}}_t$ in the time step t is obtained as:

$$\widehat{\mathbf{x}}_t = \sum_{\tau=1}^t \widehat{\mathbf{x}}_{\tau-1} + \widehat{\mathbf{o}}_\tau, \qquad \widehat{\mathbf{x}}_0 = \mathbf{x}_0 \tag{1}$$

where $\mathbf{x}_0$ is the initial pose.

Our approach decodes all poses in parallel, which contrasts with the current notion of applying autoregressive decoders [74, 71, 25]. However, using an autoregressive model is much slower during inference, and empirical evaluation showed no benefit over the proposed method in terms of quality.

Training We train our TRAJEVAE to accurately reconstruct poses, while maintaining the posterior distribution close to the prior. We achieve this by optimizing the following VAE objective [39]:

$$\mathcal{L} = \sum_{t=1}^T \mathbb{E}_{q_{\text{pose}}(\widetilde{\mathbf{z}}_t|\mathbf{x}_1, \ldots, \mathbf{x}_T)} [\log p(\widehat{\mathbf{x}}_t|\widetilde{\mathbf{z}}_t, \mathbf{x}_1, \ldots, \mathbf{x}_T)]$$
$$- \beta\text{KL}(q_{\text{pose}}(\widetilde{\mathbf{z}}_t|\mathbf{x}_1, \ldots, \mathbf{x}_T)||p_{\text{traj}}(\widehat{\mathbf{z}}_t|\mathbf{y}_1, \ldots, \mathbf{y}_T))$$

where the expectation $\mathbb{E}_{q_{\text{pose}}(\widetilde{\mathbf{z}}_t|\mathbf{x}_1,...,\mathbf{x}_T)}$ is expressed in terms of the mean squared error:

$$\mathcal{L}_{\text{MSE}} = \sum_{t=1}^{T} (\widehat{\mathbf{x}}_t - \mathbf{x}_t)^2 \qquad (2)$$

Masking future poses and data augmentation Providing target poses $\{\mathbf{x}\}_{t=1}^{T}$ during training directly leads to over-fitting and the network, in the end, is unable to match the posterior with the prior. This further degrades the quality of reconstructed poses during inference. To overcome the problem, we mask input poses $\mathbf{X}$ with the inverse mask $\mathbf{M}$, that was used to obtain trajectories, as $\mathbf{X} \odot (1 - \mathbf{M})$. This way, the pose encoder $\mathcal{E}_{\text{pose}}$ is forced to leverage the information from the prior distribution of trajectories which are structurally complementary to masked future poses.

Additionally, to improve the overall results for our 3D global coordinate representation, we propose a simple data augmentation technique that facilitates covering the data distribution of $\{\mathbf{x}\}_{t=1}^{T}$ more accurately. We achieve this by rotating the whole sequence of poses and trajectories relative to the Z axis by a random angle $\alpha \in [-\pi, \pi]$.

4. Experiments

We evaluate TRAJEVAE in two scenarios. Firstly, we evaluate the performance of our method and of several baselines when we progressively add conditioning trajectories in the input. Secondly, we compare our method with recent methods for a stochastic human generation. Finally, we perform an ablation study to validate our design decisions.

Datasets All our experiments are based on the Human3.6m [31] dataset. It consists of 3.6 million video frames of 11 subjects performing 15 actions. We follow the evaluation protocol used in [71] and hence we use 17-joint poses. The training was done on subjects S1, S5, S6, S7, S8 while subjects S9 and S11 are left for the testing. We test the baselines and our method by predicting 2 seconds of future motion.

We represent human poses and trajectories as a set of joints parametrized as global coordinates. We also normalize each sequence such that the pelvis of the initial pose is located at the $(0, 0, 0)$ coordinate.

Baselines To show the generality of our approach, we define three baselines that, thanks to our paradigm, enable generation of human motions for a variable number of trajectories. Deterministic RNN and stochastic CVAE are both derived from [71]. We also adapt MoGlow [25] to use the same data format as ours. MoGlow is a recent state-of-the-art approach for controllable human motion generation. In its original version, MoGlow only supports walking, running, and stepping. The conditioning signal used by the authors is expressed in terms of axis velocities for the pelvis joint. We use the introduced paradigm of pose completion

to extend MoGlow so that it can be applied to any other action. We provide additional implementation details of these baselines in the supplementary material.

In the second experiment, we follow the evaluation protocol of DLow [71] and use its baselines for the Human3.6M [31] dataset. In contrast to [71], our method requires only a single past frame (the initial pose) while the evaluation used by the authors assumed 25 past frames for Human3.6m.

Metrics We evaluate the methods using the *diversity* and *accuracy* metrics defined in [71]. ***Average Pairwise Distance (APD)*** describes the diversity of a set of size K of motions sampled given the same input trajectory. It is expressed as the average L_2 distance between all pairs of generated motions $\frac{1}{K(K-1)} \sum_{i=1}^{K} \sum_{j \neq i}^{K} ||\widehat{\mathbf{x}}_i - \widehat{\mathbf{x}}_j||_2$. ***Average Displacement Error (ADE)*** measures the accuracy of the reconstructed motion and calculates the average L_2 distance across all time steps between the ground truth motion and the motion from a generated set of K motions that is the closest to the ground truth $\frac{1}{T} \min_{\widehat{\mathbf{x}} \in \widehat{\mathbf{X}}} \sum_{t=1}^{T} ||\widehat{\mathbf{x}}_t - \mathbf{x}_t||_2$. ***Final Displacement Error (FDE)*** calculates the L_2 distance between the pose in the last time step of ground truth motion and the motion from a generated set of K motions that is the closest to the ground truth $\min_{\widehat{x} \in \widehat{\mathbf{X}}} ||\widehat{\mathbf{x}}_T - \mathbf{x}_T||_2$. ***Multi-Modal ADE (MMADE)*** and ***Multi-Modal FDE (MMFDE)*** calculates an average of ADE and FDE respectively between a predicted motion and all samples in the clustered ground truth. Clusters are obtained by grouping sequences where the L_2 distance between their initial poses differs by less than the user-defined ϵ.

Implementation details At the training time, we obtain masks $\mathbf{M} \supset \mathbf{m} \in \{0,1\}^{3J}$ by sampling from the Bernoulli distribution $\mathcal{B}(p_{\mathbf{m}})$ with a probability $p_{\mathbf{m}}$. Then, we replicate the $\mathbf{m}$ vector T times to create the structured mask $\mathbf{M} \in \{0,1\}^{T \times 3J}$. We set $p_{\mathbf{m}} = 0.85$ so the network sees 3 − 4 trajectories on average in the input. We find that number to be a sensible trade-off between the accuracy and effort of defining trajectories when using TRAJEVAE in practice.

We train TRAJEVAE and the corresponding baselines with the Adam optimizer [38] with learning rate set to 0.0001 and multiplied by 0.25 every 80,000 training steps. We set $\beta = 0.01$, the batch size $= 64$ and we train the model for 240,000 steps.

4.1. Qualitative results

Reconstructed sequences To visually examine the proposed method, we generate a set of poses while changing the number of input trajectories. Fig. 3 shows individual frames from selected animation sequences (refer to the supplementary material to see full video clips). When more trajectories are provided, the generated sequence resembles the ground truth more closely. However, even if no trajectory is provided, TRAJEVAE generates plausible poses. We
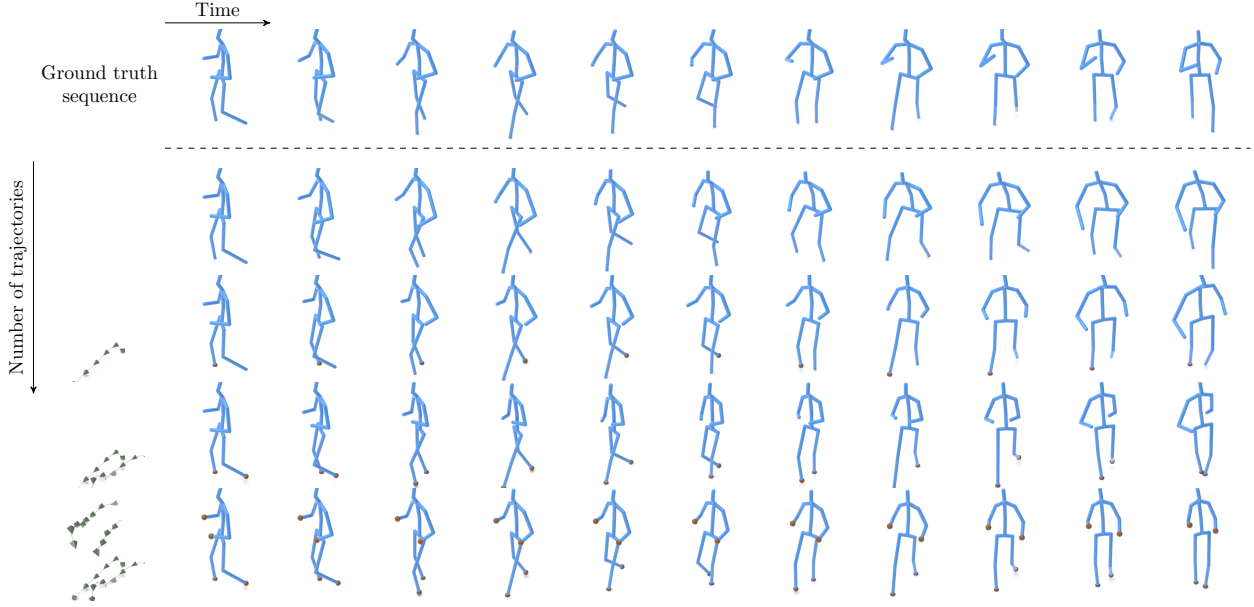
Figure 3. By using TRAJEVAE, we can provide more trajectories in the input to create a more realistic pose that follows a particular path. Joints that are not described by a trajectory are completed by our method. The joints that have a corresponding input trajectory are depicted as brown spheres. The top row shows the ground truth sequence. Rows below show generated sequences when more and more trajectories are given, in the order: right foot, left foot, right and left hands.

achieve this by providing the initial pose to the model during the decoding phase. Otherwise, the method would generate a completely random pose sequence.

Diversity vs. number of input trajectories Since TRAJEVAE allows us to sample latent DCT components from a learnable prior distribution, we can generate multiple, diverse samples for the same set of conditioning trajectories. We show the last frames of such generated samples in Fig. 4. When no trajectories are present, the method generates the most diverse outputs, while retaining the plausibility of poses. As we noticed by examining the generated sequences, such poses can represent waving, bending, or dancing-like motions. When four trajectories are given, generated poses converge towards the ground truth.

Due to the MSE term in Eq. 2, the model is not forced to exactly reproduce the trajectories, and therefore the results plateau when we provide more than ten trajectories. Applying L_1 loss instead of L_2 mitigates that issue but significantly impedes the diversity of generated samples.

Generalization Finally, we empirically prove that, in contrast to other works on controllable human motion generation, TRAJEVAE can be applied to any set of motions, *e.g.* dancing, sitting, waving, and others. As we present in Fig. 5, TRAJEVAE generalizes to a variety of different sets of motions that were not handled by previous methods. We additionally show in the supplementary, that given the same trajectory but a different initial pose, our method still generates poses that follow the provided trajectory. It confirms that our approach leverages both the initial pose and

Method	k	APD $\uparrow$	ADE $\downarrow$	FDE $\downarrow$	MMADE $\downarrow$	MMFDE $\downarrow$
TRAJEVAE		8.462	**0.518**	**0.678**	**0.596**	**0.703**
MoGlow [25]	0	1.786	0.548	0.776	0.626	0.803
RNN		0.0	0.573	0.797	0.645	0.828
CVAE-RNN		**9.579**	0.611	0.723	0.639	0.724
TRAJEVAE		6.641	**0.463**	**0.602**	**0.581**	**0.672**
MoGlow [25]	1	1.813	0.546	0.773	0.625	0.801
RNN		0.0	0.551	0.765	0.655	0.845
CVAE-RNN		**9.498**	0.603	0.733	0.647	0.753
TRAJEVAE		6.334	**0.450**	**0.581**	**0.581**	**0.668**
MoGlow [25]	2	1.861	0.544	0.768	0.623	0.797
RNN		0.0	0.540	0.738	0.661	0.845
CVAE-RNN		**9.496**	0.588	0.714	0.642	0.745
TRAJEVAE		5.037	**0.375**	**0.488**	**0.579**	**0.664**
MoGlow [25]	3	1.844	0.540	0.766	0.623	0.798
RNN		0.0	0.476	0.636	0.667	0.855
CVAE-RNN		**9.309**	0.516	0.626	0.614	0.699
TRAJEVAE		4.069	**0.325**	**0.428**	**0.584**	**0.674**
MoGlow [25]	4	1.858	0.530	0.750	0.619	0.790
RNN		0.0	0.436	0.575	0.687	0.887
CVAE-RNN		**9.242**	0.459	0.560	0.602	0.679

Table 1. Influence of the **number of trajectories** k on the quantitative results. RNN is a deterministic model and cannot produce diverse samples. Best results are in bold.

trajectories, and can be used to generate animations beyond the ones found in the dataset.

4.2. Quantitative Results

Controlling future motion prediction We evaluate the quality of generated samples while changing the number of input trajectories. We first compute the metrics with no
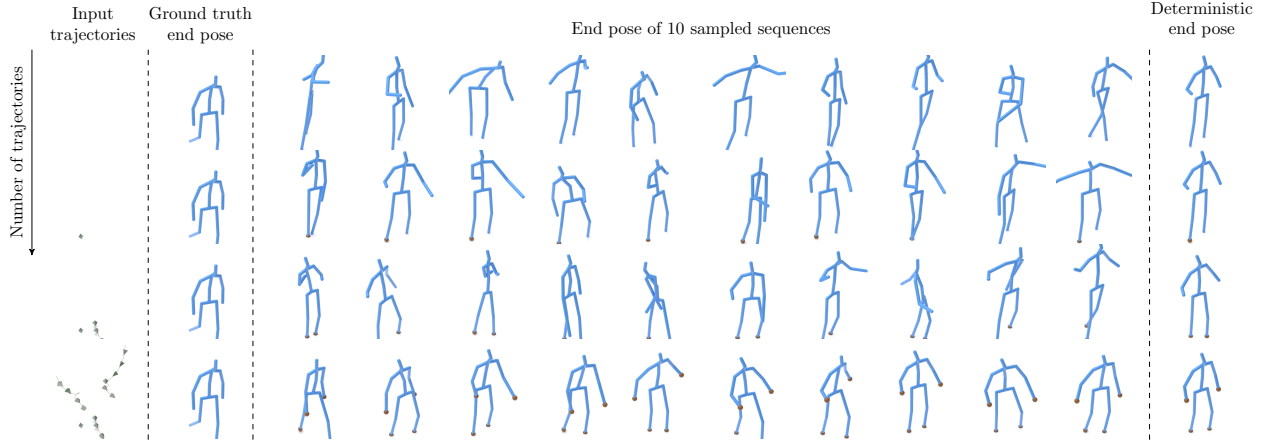
Figure 4. TRAJEVAE allows us to use a variable number of trajectories and sample multiple diverse pose sequences. We show in each row input trajectories, expected end pose for the sequence, end poses for 10 sampled sequences, and the end pose for a sequence decoded from trajectory means $\{\widehat{\mu}\}_{t=1}^{T}$. The joints that have a specified trajectory are colored in brown.
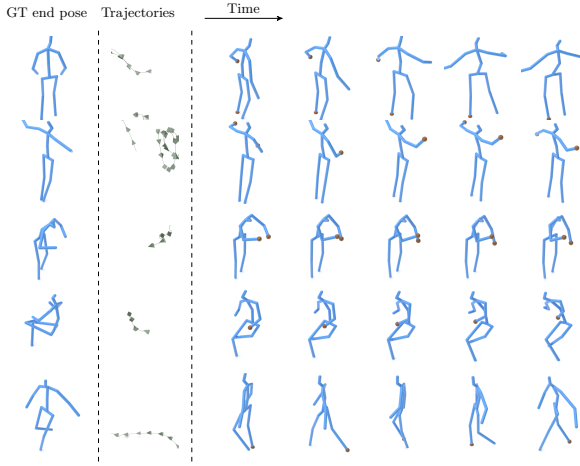

Figure 5. TRAJEVAE is not limited to only walking, running, or standing as in related works and can be applied to any motion type. Each row represents a generated sequence for a different motion class given specific trajectories. The joints that have a specified trajectory are colored in brown.
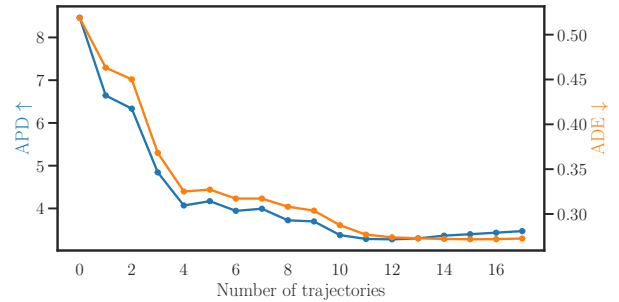

Figure 6. Providing more trajectories in the input causes that the reconstruction error (ADE) of the reconstruction decreases gradually for the cost of the decreased diversity (APD).

provided trajectories and then progressively increase their number by adding the following: right foot, left foot, right hand, and left hand. This order was based on the variance of coordinates of joints they correspond to. In each case, we sample $K = 50$ poses to calculate metrics. Results are summarized in Tab. 1. As expected, adding more trajectories decreases the diversity (APD) of samples since the pose is restricted to follow a particular path. At the same time, the accuracy (ADE) of generated samples improves. Our TRAJEVAE obtains the best results in terms of the reconstruction quality in comparison to other methods. The higher diversity of CVAE-RNN is caused by its structure. In contrast to TRAJEVAE, CVAE-RNN encodes the whole

sequence into a single latent code instead of multiple, independent components. Therefore, two samples from the prior may have a significantly different structure in the output. However, such an architecture suffers from pose averaging where most of the pose frames are the same in a generated sequence [17, 44] which leads to the inferior accuracy of the reconstructed motions.

In Fig. 6 we show that including more trajectories in the input improves the reconstruction quality. Notice that including too many trajectories plateaus the quality. We conclude that it is caused by the randomness in the latent space, and hence the network is unable to properly encode all the input trajectories to reconstruct poses accurately. Interestingly, the diversity (APD) is the lowest for ten trajectories and slightly increases when we add more trajectories. We argue that this phenomenon may be caused by the order we use when adding trajectories. The last seven trajectories break the bias in the prior, but due to their low influence on the sequence, they do not affect the quality.

Comparison with other methods for future motion generation Our method is the first one that allows generating

Method	APD ↑	ADE ↓	FDE ↓	MMADE ↓	MMFDE ↓
TRAJEVAE ($k = 0$)	8.462	0.518	0.678	0.596	0.703
TRAJEVAE ($k = 1$)	6.641	0.463	0.602	0.581	0.672
TRAJEVAE ($k = 2$)	6.334	0.450	0.581	0.581	0.668
TRAJEVAE ($k = 3$)	5.037	0.375	0.488	0.579	0.664
TRAJEVAE ($k = 4$)	4.069	**0.325**	**0.428**	0.584	0.674
DLow [71]	**11.741**	0.425	0.518	**0.495**	**0.531**
ERD [17]	0.0	0.722	0.969	0.776	0.995
acLSTM [44]	0.0	0.789	1.126	0.849	1.139
Pose-Knows [64]	6.723	0.461	0.560	0.522	0.569
MT-VAE [68]	0.403	0.457	0.595	0.716	0.883
HP-GAN [7]	7.214	0.858	0.867	0.847	0.858
Best-of-Many [9]	6.265	0.448	0.533	0.514	0.544
GMVAE [15]	6.769	0.461	0.555	0.524	0.566
DeLiGAN [23]	6.509	0.483	0.534	0.520	0.545
DSF [70]	9.330	0.493	0.592	0.550	0.599

Table 2. **Quantitative results** for the Human3.6M dataset when $K = 50$ samples are generated. For our method, we assume different scenarios when $k = \{0, 1, 2, 3, 4\}$ trajectories are provided. We explicitly delimit DLow [71] and its baselines as these methods do not use trajectories and predict future poses from 25 past frames. Best results are in bold.

Method	ADE ↓	FDE ↓
TRAJEVAE ($k = 0$)	0.529	0.779
TRAJEVAE ($k = 1$)	0.491	0.735
TRAJEVAE ($k = 2$)	0.477	0.710
TRAJEVAE ($k = 3$)	0.396	0.593
TRAJEVAE ($k = 4$)	**0.345**	**0.522**
DLow [71]	1.126	1.652

Table 3. **Quantitative results** for the Human3.6M dataset when a single future pose sequence ($K = 1$) is generated. For our method, we assume different scenarios when $k = \{0, 1, 2, 3, 4\}$ trajectories are provided. In this experiment, TRAJEVAE decodes predicted means $\{\widehat{\mu}\}_{t=1}^T$ of trajectories. Best results are in bold.

Method	APD ↑	ADE ↓	FDE ↓	MMADE ↓	MMFDE ↓
Base	1.220	0.481	0.695	0.640	0.811
+ DCT	0.849	0.485	0.711	0.649	0.836
+ Learnable prior	**7.136**	0.482	0.638	0.603	0.715
+ Data augmentation	6.735	0.469	0.622	0.594	0.700
+ Masked future poses	6.704	**0.464**	**0.607**	**0.583**	**0.675**

Table 4. Influence of design decisions on obtained results for a single given trajectory (a right foot). Best results are in bold. For the ablation study with more trajectories, refer to the supplementary.

future poses from any number of trajectories. Since there are no other known approaches enabling that, we compare TRAJEVAE with methods that generate future poses from a set of past frames. We evaluate the methods in two scenarios: when sampling $K = 50$ different poses, and when sampling only a single pose. We show results for TRAJEVAE when $k = \{0, 1, 2, 3, 4\}$ trajectories are present in the input. Results are summarized in Tab. 2 for $K = 50$ and Tab. 3 for $K = 1$.

When $K = 50$, while working on an initial pose only without a conditioning trajectory, TRAJEVAE produces poses comparable in terms of the accuracy to those generated by other approaches even though it was not trained specifically for this task. When we use $k = 3$ trajectories, the accuracy is better than for all other baselines. Note that DLow [71] uses a set of past frames as the conditioning data and therefore has more information in the input. Both DLow [71] and DSF [70] were specifically trained to generate diverse samples while TRAJEVAE implicitly provides high diversity by having a more flexible, learnable prior distribution. DLow is additionally constrained to always generate K poses and cannot be extended to more samples.

When $K = 1$, our method is capable of creating accu-

rate pose sequences for a single sample. To adapt DLow to this scenario, we take the first pose from all its K generated poses. DLow's much lower accuracy compared to experiments with $K = 50$ is caused by its diverse outputs, many of which do no match the ground truth. Since DLow does not allow for controlling the trade-off between diversity and accuracy, it is unable to generate an accurate pose sequence reliably if only a single sample is generated. In comparison, our method is capable of controlling that trade-off and thus producing accurate results even if only a single output sample is generated.

Ablation study Finally, we perform an ablation study of our design decisions: using the Discrete Cosine Transform in the latent space, making the prior distribution learnable, additional data augmentation and masking future poses with the mask $1 - \mathbf{M}$. We show obtained results in Tab. 4.

Using the DCT in the latent space does not improve results when compared to the base model. However, since the DCT uses an orthogonal basis, each obtained component is independent of others. Theoretically, it allows us to sample latent components from the normal distribution in parallel without worrying about their possible interdependence.

We also found it beneficial to apply two regularization techniques to improve results: data augmentation by performing a random rotation of the whole sequence of poses, and masking future poses with the mask $1 - \mathbf{M}$. By masking poses, the network has to learn to encode more information from poses and stops to rely entirely on the prior distribution.

5. Conclusions, limitations, and future work

We introduced the notion of trajectory-conditioned pose generation as a pose completion problem. It allowed us to define TRAJEVAE — a method for controllable and stochastic human animation generation. We showed that the paradigm of structured dropping of joints during training, creates a model that can generate realistic poses that follow an arbitrary number of trajectories. Obtained results show the applicability of our method in designing realistic human animations. While our approach trivially generalizes to other data representations, applying it to full-body parametric models, such as SMPL [51, 74], is of high importance.

We identify two limitations of our approach. Firstly, generated poses do not follow the trajectories exactly. While we could resort to a cGAN [20] model as a possible solution for its unprecedented quality of generated samples [36], the application of GANs to structured time series data is still a challenge.

Secondly, when the initial pose is ambiguous about what action it represents, TRAJEVAE tends to stretch bones when we input only a single or none trajectories. Applying exponential maps [54] constrains bone lengths but this would limit our method to only work with skeleton structures that have a clearly defined kinematic chain.

Acknowledgements

References

[1] Nasir Ahmed, T. Natarajan, and Kamisetty R Rao. Discrete cosine transform. *IEEE transactions on Computers*, 100(1):90–93, 1974. 2, 4

[2] Emre Aksan, Peng Cao, Manuel Kaufmann, and Otmar Hilliges. Attention, please: A spatio-temporal transformer for 3d human motion prediction. *arXiv preprint arXiv:2004.08692*, 2020. 2

[3] Emre Aksan, Manuel Kaufmann, and Otmar Hilliges. Structured prediction helps 3d human motion modelling. In *Proceedings of the IEEE/CVF International Conference on Computer Vision*, pages 7144–7153, 2019. 2

[4] Sadegh Aliakbarian, Fatemeh Sadat Saleh, Lars Petersson, Stephen Gould, and Mathieu Salzmann. Contextually plausible and diverse 3d human motion prediction. *arXiv preprint arXiv:1912.08521*, 2019. 2

[5] Andreas Aristidou, Joan Lasenby, Yiorgos Chrysanthou, and Ariel Shamir. Inverse kinematics techniques in computer graphics: A survey. In *Computer Graphics Forum*, volume 37, pages 35–58. Wiley Online Library, 2018. 1

[6] Martin Arjovsky, Soumith Chintala, and Léon Bottou. Wasserstein generative adversarial networks. In *International conference on machine learning*, pages 214–223. PMLR, 2017. 2

[7] Emad Barsoum, John Kender, and Zicheng Liu. Hp-gan: Probabilistic 3d human motion prediction via gan. In *Proceedings of the IEEE conference on computer vision and pattern recognition workshops*, pages 1418–1427, 2018. 2, 8

[8] Marcelo Bertalmio, Guillermo Sapiro, Vincent Caselles, and Coloma Ballester. Image inpainting. In *Proceedings of the 27th annual conference on Computer graphics and interactive techniques*, pages 417–424, 2000. 3

[9] Apratim Bhattacharyya, Bernt Schiele, and Mario Fritz. Accurate and diverse sampling of sequences based on a "best of many" sample objective. In *Proceedings of the IEEE Conference on Computer Vision and Pattern Recognition*, pages 8485–8493, 2018. 8

[10] Weiwei Cai and Zhanguo Wei. Piigan: Generative adversarial networks for pluralistic image inpainting. *IEEE Access*, 8:48451–48463, 2020. 3

[11] Yujun Cai, Lin Huang, Yiwei Wang, Tat-Jen Cham, Jianfei Cai, Junsong Yuan, Jun Liu, Xu Yang, Yiheng Zhu, Xiaohui Shen, et al. Learning progressive joint propagation for human motion prediction. In *European Conference on Computer Vision*, pages 226–242. Springer, 2020. 2

[12] Wenheng Chen, He Wang, Yi Yuan, Tianjia Shao, and Kun Zhou. Dynamic future net: Diversified human motion generation. In *Proceedings of the 28th ACM International Conference on Multimedia*, pages 2131–2139, 2020. 2, 3

[13] Qiongjie Cui, Huaijiang Sun, and Fei Yang. Learning dynamic relationships for 3d human motion prediction. In *Proceedings of the IEEE/CVF Conference on Computer Vision and Pattern Recognition*, pages 6519–6527, 2020. 2

[14] Emily Denton and Rob Fergus. Stochastic video generation with a learned prior. In *International Conference on Machine Learning*, pages 1174–1183. PMLR, 2018. 4

[15] Nat Dilokthanakul, Pedro AM Mediano, Marta Garnelo, Matthew CH Lee, Hugh Salimbeni, Kai Arulkumaran, and Murray Shanahan. Deep unsupervised clustering with gaussian mixture variational autoencoders. *arXiv preprint arXiv:1611.02648*, 2016. 2, 8

[16] Marek Dvorožňák, Daniel Sỳkora, Cassidy Curtis, Brian Curless, Olga Sorkine-Hornung, and David Salesin. Monster mash: a single-view approach to casual 3d modeling and animation. *ACM Transactions on Graphics (TOG)*, 39(6):1–12, 2020. 3

[17] Katerina Fragkiadaki, Sergey Levine, Panna Felsen, and Jitendra Malik. Recurrent network models for human dynamics. In *Proceedings of the IEEE International Conference on Computer Vision*, pages 4346–4354, 2015. 2, 7, 8

[18] Saeed Ghorbani, Calden Wloka, Ali Etemad, Marcus A Brubaker, and Nikolaus F Troje. Probabilistic character motion synthesis using a hierarchical deep latent variable model. In *Computer Graphics Forum*, volume 39, pages 225–239. Wiley Online Library, 2020. 2

[19] Partha Ghosh, Jie Song, Emre Aksan, and Otmar Hilliges. Learning human motion models for long-term predictions. In *2017 International Conference on 3D Vision (3DV)*, pages 458–466. IEEE, 2017. 2

[20] Ian J Goodfellow, Jean Pouget-Abadie, Mehdi Mirza, Bing Xu, David Warde-Farley, Sherjil Ozair, Aaron Courville, and Yoshua Bengio. Generative adversarial networks. *arXiv preprint arXiv:1406.2661*, 2014. 2, 3, 9

[21] Anand Gopalakrishnan, Ankur Mali, Dan Kifer, Lee Giles, and Alexander G Ororbia. A neural temporal model for human motion prediction. In *Proceedings of the IEEE/CVF Conference on Computer Vision and Pattern Recognition*, pages 12116–12125, 2019. 2

[22] Liang-Yan Gui, Yu-Xiong Wang, Xiaodan Liang, and José MF Moura. Adversarial geometry-aware human motion prediction. In *Proceedings of the European Conference on Computer Vision (ECCV)*, pages 786–803, 2018. 2

[23] Swaminathan Gurumurthy, Ravi Kiran Sarvadevabhatla, and R Venkatesh Babu. Deligan: Generative adversarial networks for diverse and limited data. In *Proceedings of the IEEE conference on computer vision and pattern recognition*, pages 166–174, 2017. 2, 8

[24] Felix G Harvey, Julien Roy, David Kanaa, and Christopher Pal. Recurrent semi-supervised classification and constrained adversarial generation with motion capture data. *Image and Vision Computing*, 78:42–52, 2018. 2

[25] Gustav Eje Henter, Simon Alexanderson, and Jonas Beskow. Moglow: Probabilistic and controllable motion synthesis using normalising flows. *ACM Transactions on Graphics (TOG)*, 39(6):1–14, 2020. 2, 3, 4, 5, 6, 12

[26] Alejandro Hernandez, Jurgen Gall, and Francesc Moreno-Noguer. Human motion prediction via spatio-temporal inpainting. In *Proceedings of the IEEE/CVF International Conference on Computer Vision*, pages 7134–7143, 2019. 2, 3

[27] Daniel Holden, Oussama Kanoun, Maksym Perepichka, and Tiberiu Popa. Learned motion matching. *ACM Transactions on Graphics (TOG)*, 39(4):53–1, 2020. 1

[28] Daniel Holden, Taku Komura, and Jun Saito. Phase-functioned neural networks for character control. *ACM Transactions on Graphics (TOG)*, 36(4):1–13, 2017. 2, 3

[29] Daniel Holden, Jun Saito, and Taku Komura. A deep learning framework for character motion synthesis and editing. *ACM Transactions on Graphics (TOG)*, 35(4):1–11, 2016. 2

[30] Daniel Holden, Jun Saito, Taku Komura, and Thomas Joyce. Learning motion manifolds with convolutional autoencoders. In *SIGGRAPH Asia 2015 Technical Briefs*, pages 1–4. 2015. 2

[31] Catalin Ionescu, Dragos Papava, Vlad Olaru, and Cristian Sminchisescu. Human3. 6m: Large scale datasets and predictive methods for 3d human sensing in natural environments. *IEEE transactions on pattern analysis and machine intelligence*, 36(7):1325–1339, 2013. 5

[32] Karim Iskakov, Egor Burkov, Victor Lempitsky, and Yury Malkov. Learnable triangulation of human pose. In *Proceedings of the IEEE/CVF International Conference on Computer Vision*, pages 7718–7727, 2019. 2

[33] Deok-Kyeong Jang and Sung-Hee Lee. Constructing human motion manifold with sequential networks. In *Computer Graphics Forum*, volume 39, pages 314–324. Wiley Online Library, 2020. 2

[34] Gunnar Johansson. Visual perception of biological motion and a model for its analysis. *Perception & psychophysics*, 14(2):201–211, 1973. 2

[35] Angjoo Kanazawa, Jason Y Zhang, Panna Felsen, and Jitendra Malik. Learning 3d human dynamics from video. In *Proceedings of the IEEE/CVF Conference on Computer Vision and Pattern Recognition*, pages 5614–5623, 2019. 2

[36] Tero Karras, Samuli Laine, and Timo Aila. A style-based generator architecture for generative adversarial networks. In *Proceedings of the IEEE/CVF Conference on Computer Vision and Pattern Recognition*, pages 4401–4410, 2019. 9

[37] Manuel Kaufmann, Emre Aksan, Jie Song, Fabrizio Pece, Remo Ziegler, and Otmar Hilliges. Convolutional autoencoders for human motion infilling. *arXiv preprint arXiv:2010.11531*, 2020. 2

[38] Diederik P. Kingma and Jimmy Ba. Adam: A method for stochastic optimization. In Yoshua Bengio and Yann LeCun, editors, *3rd International Conference on Learning Representations, ICLR 2015, San Diego, CA, USA, May 7-9, 2015, Conference Track Proceedings*, 2015. 5, 12

[39] Diederik P Kingma and Max Welling. Auto-encoding variational bayes. *arXiv preprint arXiv:1312.6114*, 2013. 2, 4

[40] Jogendra Nath Kundu, Maharshi Gor, and R Venkatesh Babu. Bihmp-gan: Bidirectional 3d human motion prediction gan. In *Proceedings of the AAAI conference on artificial intelligence*, volume 33, pages 8553–8560, 2019. 2

[41] Tim Lebailly, Sena Kiciroglu, Mathieu Salzmann, Pascal Fua, and Wei Wang. Motion prediction using temporal inception module. In *Proceedings of the Asian Conference on Computer Vision*, 2020. 2

[42] Chen Li, Zhen Zhang, Wee Sun Lee, and Gim Hee Lee. Convolutional sequence to sequence model for human dynamics. In *Proceedings of the IEEE Conference on Computer Vision and Pattern Recognition*, pages 5226–5234, 2018. 2

[43] Maosen Li, Siheng Chen, Yangheng Zhao, Ya Zhang, Yanfeng Wang, and Qi Tian. Dynamic multiscale graph neural networks for 3d skeleton based human motion prediction. In *Proceedings of the IEEE/CVF Conference on Computer Vision and Pattern Recognition*, pages 214–223, 2020. 2

[44] Zimo Li, Yi Zhou, Shuangjiu Xiao, Chong He, Zeng Huang, and Hao Li. Auto-conditioned recurrent networks for extended complex human motion synthesis. *arXiv preprint arXiv:1707.05363*, 2017. 2, 7, 8

[45] Xiao Lin and Mohamed R Amer. Human motion modeling using dvgans. *arXiv preprint arXiv:1804.10652*, 2018. 2

[46] Guilin Liu, Fitsum A Reda, Kevin J Shih, Ting-Chun Wang, Andrew Tao, and Bryan Catanzaro. Image inpainting for irregular holes using partial convolutions. In *Proceedings of the European Conference on Computer Vision (ECCV)*, pages 85–100, 2018. 3

[47] Wei Mao, Miaomiao Liu, and Mathieu Salzmann. History repeats itself: Human motion prediction via motion attention. In *European Conference on Computer Vision*, pages 474–489. Springer, 2020. 2

[48] Wei Mao, Miaomiao Liu, Mathieu Salzmann, and Hongdong Li. Learning trajectory dependencies for human motion prediction. In *Proceedings of the IEEE/CVF International Conference on Computer Vision*, pages 9489–9497, 2019. 2

[49] Julieta Martinez, Michael J Black, and Javier Romero. On human motion prediction using recurrent neural networks. In *Proceedings of the IEEE Conference on Computer Vision and Pattern Recognition*, pages 2891–2900, 2017. 2

[50] Kamyar Nazeri, Eric Ng, Tony Joseph, Faisal Z Qureshi, and Mehran Ebrahimi. Edgeconnect: Generative image inpainting with adversarial edge learning. *arXiv preprint arXiv:1901.00212*, 2019. 3

[51] Georgios Pavlakos, Vasileios Choutas, Nima Ghorbani, Timo Bolkart, Ahmed AA Osman, Dimitrios Tzionas, and Michael J Black. Expressive body capture: 3d hands, face, and body from a single image. In *Proceedings of the IEEE/CVF Conference on Computer Vision and Pattern Recognition*, pages 10975–10985, 2019. 8

[52] Dario Pavllo, Christoph Feichtenhofer, Michael Auli, and David Grangier. Modeling human motion with quaternion-

based neural networks. *International Journal of Computer Vision*, pages 1–18, 2019. 2, 3

[53] Dario Pavllo, Christoph Feichtenhofer, David Grangier, and Michael Auli. 3d human pose estimation in video with temporal convolutions and semi-supervised training. In *Proceedings of the IEEE/CVF Conference on Computer Vision and Pattern Recognition*, pages 7753–7762, 2019. 2, 3

[54] Dario Pavllo, David Grangier, and Michael Auli. Quaternet: A quaternion-based recurrent model for human motion. *arXiv preprint arXiv:1805.06485*, 2018. 2, 3, 9

[55] Donald L Peiper. The kinematics of manipulators under computer control. Technical report, Stanford univ ca dept of computer science, 1968. 1

[56] Danilo Rezende and Shakir Mohamed. Variational inference with normalizing flows. In *International Conference on Machine Learning*, pages 1530–1538. PMLR, 2015. 2

[57] Charles Rose, Michael F Cohen, and Bobby Bodenheimer. Verbs and adverbs: Multidimensional motion interpolation. *IEEE Computer Graphics and Applications*, 18(5):32–40, 1998. 2

[58] Charles F Rose III, Peter-Pike J Sloan, and Michael F Cohen. Artist-directed inverse-kinematics using radial basis function interpolation. In *Computer Graphics Forum*, volume 20, pages 239–250. Wiley Online Library, 2001. 2

[59] Sebastian Starke, He Zhang, Taku Komura, and Jun Saito. Neural state machine for character-scene interactions. *ACM Trans. Graph.*, 38(6):209–1, 2019. 3

[60] Christian Szegedy, Wei Liu, Yangqing Jia, Pierre Sermanet, Scott Reed, Dragomir Anguelov, Dumitru Erhan, Vincent Vanhoucke, and Andrew Rabinovich. Going deeper with convolutions. In *Proceedings of the IEEE conference on computer vision and pattern recognition*, pages 1–9, 2015. 2

[61] Yongyi Tang, Lin Ma, Wei Liu, and Weishi Zheng. Long-term human motion prediction by modeling motion context and enhancing motion dynamic. *arXiv preprint arXiv:1805.02513*, 2018. 2

[62] Graham W Taylor, Geoffrey E Hinton, and Sam T Roweis. Modeling human motion using binary latent variables. In *Advances in neural information processing systems*, pages 1345–1352. Citeseer, 2007. 2

[63] Ashish Vaswani, Noam Shazeer, Niki Parmar, Jakob Uszkoreit, Llion Jones, Aidan N Gomez, Lukasz Kaiser, and Illia Polosukhin. Attention is all you need. *arXiv preprint arXiv:1706.03762*, 2017. 4, 12

[64] Jacob Walker, Kenneth Marino, Abhinav Gupta, and Martial Hebert. The pose knows: Video forecasting by generating pose futures. In *Proceedings of the IEEE international conference on computer vision*, pages 3332–3341, 2017. 2, 8

[65] Tianming Wang and Xiaojun Wan. T-cvae: Transformer-based conditioned variational autoencoder for story completion. In *IJCAI*, pages 5233–5239, 2019. 4

[66] Zhiyong Wang, Jinxiang Chai, and Shihong Xia. Combining recurrent neural networks and adversarial training for human motion synthesis and control. *IEEE transactions on visualization and computer graphics*, 27(1):14–28, 2019. 2

[67] Wei Xiong, Jiahui Yu, Zhe Lin, Jimei Yang, Xin Lu, Connelly Barnes, and Jiebo Luo. Foreground-aware image inpainting. In *Proceedings of the IEEE/CVF Conference on Computer Vision and Pattern Recognition*, pages 5840–5848, 2019. 3

[68] Xinchen Yan, Akash Rastogi, Ruben Villegas, Kalyan Sunkavalli, Eli Shechtman, Sunil Hadap, Ersin Yumer, and Honglak Lee. Mt-vae: Learning motion transformations to generate multimodal human dynamics. In *Proceedings of the European Conference on Computer Vision (ECCV)*, pages 265–281, 2018. 2, 8

[69] Jiahui Yu, Zhe Lin, Jimei Yang, Xiaohui Shen, Xin Lu, and Thomas S Huang. Generative image inpainting with contextual attention. In *Proceedings of the IEEE conference on computer vision and pattern recognition*, pages 5505–5514, 2018. 3

[70] Ye Yuan and Kris Kitani. Diverse trajectory forecasting with determinantal point processes. *arXiv preprint arXiv:1907.04967*, 2019. 2, 8

[71] Ye Yuan and Kris Kitani. Dlow: Diversifying latent flows for diverse human motion prediction. In *European Conference on Computer Vision*, pages 346–364. Springer, 2020. 2, 3, 4, 5, 8, 12

[72] He Zhang, Sebastian Starke, Taku Komura, and Jun Saito. Mode-adaptive neural networks for quadruped motion control. *ACM Transactions on Graphics (TOG)*, 37(4):1–11, 2018. 2, 3

[73] Jason Y Zhang, Panna Felsen, Angjoo Kanazawa, and Jitendra Malik. Predicting 3d human dynamics from video. In *Proceedings of the IEEE/CVF International Conference on Computer Vision*, pages 7114–7123, 2019. 2

[74] Yan Zhang, Michael J Black, and Siyu Tang. We are more than our joints: Predicting how 3d bodies move. *arXiv preprint arXiv:2012.00619*, 2020. 2, 4, 8

[75] Chuanxia Zheng, Tat-Jen Cham, and Jianfei Cai. Pluralistic image completion. In *Proceedings of the IEEE/CVF Conference on Computer Vision and Pattern Recognition*, pages 1438–1447, 2019. 2, 3, 4

A. Adapting MoGlow

As mentioned in the main text, MoGlow [25] conditions predicted poses on a *control signal*. This signal represents relative and rotational velocities on the ground plane. Moreover, the authors use the exponential map representation but at the same time claim that MoGlow can be used for any other well-known skeleton representation. We identify the following changes to the original implementation[1] that enabled us to use MoGlow in our framework:

1. We change the exponential map representation to the 3D coordinates of J joints.

2. We replace the control signal represented as velocities into trajectories defined as poses with some of the joints set to 0. This increases the input signal's dimensionality from $3T$ to $3JT$ for T time steps. However, it has a negligible effect on the performance.

3. We also removed regularization techniques such as gradient norm clipping and gradient value clipping and disabled data normalization. These techniques deteriorate the learning, and the network does not converge in our scenario.

4. For consistency with other methods, we use the Adam optimizer [38] with the same learning rate regime.

We left the rest of the implementation unchanged.

B. Implementation details

TRAJEVAE MLPs applied in the input and in the CVAE's bottleneck output latent codes of size 256. Therefore, vectors $\widehat{\mathbf{H}}$ and $\widetilde{\mathbf{H}}$ processed by self-attention layers have a dimensionality 512. The initial layer in the decoder $\mathcal{D}$ processes $\{[\mathbf{w}_t; \mathbf{w}_0]\}$ and is defined as a function: $f : \mathbb{R}^{768} \rightarrow \mathbb{R}^{512}$. The final layers outputs vectors of size $3J$.

All MLPs responsible for encoding poses and trajectories mentioned in the main text consists of the following structure: `Linear` → `Layer Normalization` → `Leaky ReLU`(α=0.1) → `Linear` → `Layer Normalization` → `Leaky ReLU`(α=0.1), where α is a scale of the negative slope of the function. The initial MLP in the decoder $\mathcal{D}$ has the structure `Linear` → `Layer Normalization` → `Leaky ReLU`(α=0.1) → `Linear`.

RNN and CVAE baselines operate with the same dimensionalities as TRAJEVAE. We implement them in the same way as defined in [71]. Both models use GRU networks to encode the temporal data. The recurrent decoder also receives a coordinate of the trajectory $\mathbf{y}_t$ in the time step t.

We additionally apply dropout $= 0.1$ to self-attention layers as described in [63].

---

[1]Code can be found here: https://github.com/simonalexanderson/StyleGestures

C. Same pose, different trajectories

We perform an additional experiment that confirms the generality of our approach. We show results for a scenario when we use different trajectories for the same initial pose. As expected, the generated poses follow different trajectories even though such combinations do not occur in the dataset.

Preparing the data To maintain plausibility that a particular initial pose is physically capable of following a conditioning trajectory, we pair each initial pose $\mathbf{x}_0$ in the dataset with all trajectories where the distance between $\mathbf{x}_0$ and coordinates of the trajectory in a time step $t = 0$ is below $\epsilon_0 = 0.01$. Since obtaining the ground truth sequence $\mathbf{X}$ in such a case is not possible, we assume that the sequence $\mathbf{X}$ corresponding to a given trajectory is a sufficient approximation of the expected sequence. We evaluate TRAJEVAE as previously using APD, ADE, FDE. We omit MMADE and MMFDE for its exponential computational complexity that this scenario creates.

Results We present results in Tab. 5. Even though these trajectories do not come from the same sequence as the initial poses, TRAJEVAE generates a sequence that follows the trajectory. The decrease in accuracy (ADE) between $k = 2$ and $k = 3$ is caused by adding a trajectory that corresponds to the right hand, while $k < 2$ we add only trajectories regarding feet. While feet commonly behave similarly throughout the animation, hands have a significantly different motion from other joints.

The value $k = 0$ corresponds to no trajectories, and therefore we omit it in the Tab. 5. Refer to supplementary files to find animations generated for initial poses with different trajectories.

k	APD	ADE	FDE
1	5.373	0.370	0.476
2	5.400	0.362	0.472
3	5.096	0.375	0.491
4	4.175	0.332	0.433

Table 5. **Quantitative results** for the Human3.6M dataset when $K = 50$ samples are generated for the scenario where we use different trajectories from the whole dataset for the same initial pose. We assume different situations that $k = \{1, 2, 3, 4\}$ trajectories are provided.

D. Extended ablation study

In experiments, we provide results for an ablation study when only a trajectory for the right foot is provided. We additionally show in Tab. 6 results when we input no trajectories, or progressively add trajectories of the right foot, left foot, right hand, and left hand. The extended results show that our design decisions consistently affect scenarios when we vary the number of the input trajectories.

Method	k	APD $\uparrow$	ADE $\downarrow$	FDE $\downarrow$	MMADE $\downarrow$	MMFDE $\downarrow$
Base		1.237	0.525	0.749	0.634	0.801
+ DCT		0.882	0.525	0.758	0.633	0.806
+ Learnable prior	0	**9.762**	0.569	0.768	0.640	0.787
+ Data augmentation		8.487	0.532	0.709	0.609	0.732
+ Masked future poses		8.685	**0.522**	**0.685**	**0.599**	**0.707**
Base		1.220	0.481	0.695	0.640	0.811
+ DCT		0.849	0.485	0.711	0.649	0.836
+ Learnable prior	1	**7.136**	0.482	0.638	0.603	0.715
+ Data augmentation		6.735	0.469	0.622	0.594	0.700
+ Masked future poses		6.704	**0.464**	**0.607**	**0.583**	**0.675**
Base		1.217	0.466	0.672	0.642	0.812
+ DCT		0.833	0.463	0.678	0.647	0.832
+ Learnable prior	2	**6.601**	0.456	0.597	0.596	0.699
+ Data augmentation		6.306	0.447	0.587	0.590	0.689
+ Masked future poses		6.278	**0.445**	**0.579**	**0.580**	**0.670**
Base		1.248	0.376	0.549	0.639	0.802
+ DCT		0.841	0.385	0.565	0.651	0.834
+ Learnable prior	3	**5.573**	0.385	0.508	0.595	0.692
+ Data augmentation		5.152	0.371	0.490	0.593	0.686
+ Masked future poses		4.814	**0.362**	**0.472**	**0.580**	**0.667**
Base		1.261	0.339	0.498	0.641	0.805
+ DCT		0.838	0.351	0.517	0.654	0.839
+ Learnable prior	4	**4.677**	0.335	0.450	0.603	0.702
+ Data augmentation		4.428	0.324	0.433	0.600	0.697
+ Masked future poses		3.925	**0.315**	**0.415**	**0.591**	**0.684**

Table 6. Influence of design decisions on obtained results for $k = \{0, 1, 2, 3, 4\}$ trajectories. These trajectories refer to scenarios when we use no trajectories and then add progressively trajectories for the right foot, left foot, right hand, and left hand. The best results are in bold.